meteorites is the sum of the $H^3$ and direct $He^3$ production. The ratio of directly produced $He^3$ to $H^3$ for 340-Mev protons on iron[18] is 0.6. This ratio increases with energy but cannot exceed 1.0. We shall use 0.8 at 1 Bev and 1.0 at 6 Bev. The $He^3$ to $A^{36}$ ratio is then 0.9 $H^3/A^{37}$ at 1 Bev and equal to the $H^3/A^{37}$ ratio at 6 Bev. With this correction factor the $He^3/A^{36}$ in meteorites for 1-Bev particles should be about 14 and for 6-Bev particles should be about 30 for small depths and decrease to 20 at about 20 cm depth. The measured $He^3/A^{36}$ ratios for the four iron meteorites favor the 6-Bev irradiation.

[18] Martin, Thomson, Wardle, and Mayne, Phil. Mag. 45, 410 (1954).

ACKNOWLEDGMENTS

The authors are indebted to the Brookhaven Cosmotron staff, the Berkeley Bevatron staff, and the Harvard cyclotron staff for the irradiations. We are grateful to Dr. L. Winsberg for his help in the 6.2-Bev irradiation and flux calibration. And we would like to thank Dr. G. Friedlander for many discussions and Professor Fred L. Whipple for his encouragement and support.

PHYSICAL REVIEW VOLUME 107, NUMBER 6 SEPTEMBER 15, 1957

# Interaction of $K^+$ Mesons in the Interval 30–65 Mev*

T. F. HOANG,† M. F. KAPLON, AND R. CESTER‡
*Department of Physics, University of Rochester, Rochester, New York*
(Received June 6, 1957)

A systematic study of the scattering of 1173 definitely identified $K_L$ mesons and 279 $\tau$ (including $\tau'$) mesons has been made in the energy interval 30–65 Mev using photoemulsion exposed to the Berkeley $K^+$ meson beam. All scatterings of $K^+$ mesons having a projected angle greater than 2° on the emulsion plane were recorded and analyzed. The results of analysis are the following: (1) the interaction properties of the $K_L$ and $\tau$ mesons are essentially indistinguishable; (2) the coherent nuclear scattering of $K^+$ mesons interferes constructively with the Coulomb scattering; (3) in terms of the optical model, the best fit for coherent scattering corresponds to a real potential of $\sim+15$ Mev, and the inelastic scattering gives an imaginary potential of $\sim3.6$ Mev; (4) charge exchange is rare in this energy region: $\sigma$(charge exchange)/$\sigma$(incoherent) $<\frac{1}{10}$. A tentative interpretation of the results in terms of states of isotopic spin $T=0$ and $T=1$ is presented. A discussion is also given on the characteristic features of $K^+$ stars.

## I. INTRODUCTION

In the past two years a large amount of experimental data on $K^+$ mesons has been obtained by different laboratories utilizing artificially produced $K^+$ mesons. The data have been related to the intrinsic properties of the $K^+$ mesons, such as mass, lifetime, spin, and parity. However, the present status of our knowledge about the nuclear interaction properties of these particles is still incomplete. With the advent of the hydrogen bubble chamber, it is now possible to attempt a direct investigation of the $K^+-p$ interaction, and yet, at the present stage, in lieu of any $K^+-d$ investigations, information relevant to the $K^+-n$ interaction can only be obtained through a study of $K^+$ nuclei interactions. An experimental tool quite useful for this purpose is nuclear emulsion.

A general survey on the properties of the interactions of $K^+$ mesons has been presented at the Sixth Rochester Conference by Goldhaber and Dallaporta.[1] Since then, a considerable wealth of new data has been accumulated by different groups working with artificially produced $K^+$ mesons: Bologna,[2] Bristol,[3] Göttingen,[4] Padova,[5] Berkeley,[6] M.I.T. and Harvard,[7] Brookhaven,[8] and Rochester.[9]

The difficult problem which is posed in the use of photoemulsion for the investigation of the $K^+$ inter-

* Supported in part by the U. S. Atomic Energy Commission and the Office of Scientific Research of the U. S. Air Force.

† Maître de Recherches au Centre National de la Recherche Scientifique, Paris, on leave from Laboratorie LePrince-Ringuet, Ecole Polytechnique, Paris, France.

‡ Now at Istituto di Fisica, Turino, Italy.

[1] S. Goldhaber and N. Dallaporta, *Proceedings of the Sixth Annual Rochester Conference on High-Energy Physics* (Interscience Publishers, Inc., New York, 1956), Chap. VI, pp. 2 ff. and pp. 11 ff.

[2] Marchi, Pedretti, and Standic, Nuovo cimento 4, 940 (1956); Cocconi, Puppi, Quareni, and Stanghellini, Nuovo cimento 5, 172 (1956).

[3] Bhomik, Evans, Nilson, Prowse, and Harden, K2 Stack Collaboration Report (unpublished).

[4] Biswas, Ceccarelli-Fabrichesi, Ceccarelli, Gottstein, Varsheya, and Waleschek, Nuovo cimento 5, 123 (1957).

[5] Baldo-Ceolin, Cresti, Dallaporta, Grilli, Guerriers, Merlin, Salandin, and Zago, Nuovo cimento 5, 402 (1957).

[6] Lannutti, Chupp, Goldhaber, and Goldhaber, Bull. Am. Phys. Soc. Ser. II, 1, 392 (1956); Ser. II, 2, 222 (1957).

[7] Ritson, Fournet-Davis, Schluter, Pevsner, Widgoff, and Henri, Bull. Am. Phys. Soc. Ser. II, 2, 20 (1957); D. Fournet-Davis (to be published).

[8] B. Sechi-Zorn and G. T. Zorn, Bull. Am. Phys. Soc. Ser. II, 2, 20 (1957).

[9] Hoang, Kaplon, and Cester, Bull. Am. Phys. Soc. Ser. II, 2, 20 (1957).

action is to separate the nuclear scattering from the Coulomb scattering: the latter plays an important role due to the high proportion of heavy elements, Br and Ag, constituting the emulsion. The usual procedure employed to overcome this difficulty involves the use of an *a priori* cutoff to eliminate the Coulomb scattering; with this procedure, large scattering angles only are accepted in the region where the contribution due to the Coulomb scattering is thought to be small. However, this method of approach does not seem quite satisfactory; for if one attempts further to make a thorough investigation of the elastic nuclear scattering, in this case, the majority of the scattering angles are actually in the forward direction.

In the study presented here of the $K^+$ interaction an attempt is made to analyze all scattering angles of $K^+$ mesons in their passage through the emulsion without introducing any drastic cutoff. The results thus obtained in the energy region between 30 and 65 Mev are presented in this paper. The scattering data will be discussed, together with some tentative interpretation of our results.

## II. EXPERIMENTAL DETAILS

We have used a stack of Ilford G-5 stripped emulsions composed of 60 pellicles 4 in.$\times$6 in.$\times$400 $\mu$. The emulsions were packed and aligned by using the technique described in a previous publication.[10] The stack was exposed to the Berkeley 90° $K^+$ meson beam with the 4-in. side in the vertical direction and facing the beam. The momentum of the beam at the center of the stack was set at 350 Mev/$c$, with a momentum gradient about 6 Mev/$c$ per cm.[11] The emulsions were processed by the usual temperature method.

Twenty-four emulsions in the middle of the stack were used for the scanning. The $K^+$ mesons were picked up by a systematic "on-track" scan. All tracks at 2 cm from the 4-in. entrance edge, situated at least 1.5 cm in from the 6-in. horizontal edge of the emulsion, and having an *ad hoc* ionization (around twice minimum by simple inspection) were followed until they came to rest or had exceeded their expected range by 2 cm. 1273 $K$ mesons were found, all having been definitely identified as $K^+$ by their decay secondaries; they represented about 70% of all tracks followed.

A rough mass determination by ionization range has been made on 100 ending tracks having no visible decay found in 5 emulsions during the systematic "on-track" scan. About 300 grains were counted on each track at a residual range around 3 cm; the identification of the track was directly referred to a group of definitely identified $K$'s found in the same emulsion. Whenever any ambiguity arose in the identification of a track, a more refined measurement was carried out, and, if necessary, a $P\beta$ measurement was also made as a check. Among 100 tracks thus analyzed, twenty-three were identified as $K_\rho$ mesons (i.e., $K$ mesons with no visible secondaries). This indicates that the efficiency for detecting minimum secondaries in the present stack is actually about 90%, and that the proton contamination is about 25%.

During the course of the scanning, all scatterings with a projected angle greater than 2° in the emulsion plane were recorded and their spatial angles were then measured. The technique used consisted of following the track along a hair line of an eyepiece which was associated with a protractor graduated in degrees, the diameter of the field being 700 $\mu$. Any deviation of the track from the hairline can thus be easily noticed and a projected angle greater than 4° can be detected with an efficiency attaining almost 100%.

Special attention was paid to all tracks which (a) suffered a larger angle scattering, and had no visible decay at rest, (b) disappeared during the following, or (c) produced a star. In the latter case, an analysis was also made on the nature of the emitted prongs. The results are summarized in Table I.

Since the number of these tracks which have suffered a scattering is only a small fraction compared to the number of definitely identified $K^+$ tracks, we feel safe in excluding these cases in the analysis of elastic scatterings. Henceforth we shall limit ourselves to those $K^+$ mesons which were definitely identified by their decay secondaries.

## III. ELASTIC SCATTERING DATA OF $K_L$ MESONS

The criteria we have adopted for the acceptance of an "elastic" scattering are the following: (1) no visible recoil or $\beta$ ray at the vertex, (2) no detectable change in ionization before and after the scattering, and (3) overall range compatible with the expected momentum. The lower limit of energy loss thus detected due to (2) is about 5 Mev. Consequently, any scattering classified as "elastic" according to our criteria can also be an inelastic one with a small energy loss which escapes experimental detection.

TABLE I. Identification of tracks not identifiable as $K^+$ via observation of decay.

| | Identified as $K_\rho$ | Identified as proton |
|---|---|---|
| Tracks having scattering angle $>5°$ for $R>3$ mm and ending in emulsion (no secondary at ending) | 17 | 20 |
| Tracks leaving the stack after scattering | 7 | 26 |
| Disappearances | 4 | 7 |
| Tracks leading to a star (having at least 2 prongs) | 0 | 34 |

[10] Hoang, Kaplon, and Yekutieli, Phys. Rev. **105**, 278 (1956).

[11] For the characteristics of the Berkeley 90° $K^+$ beam, we refer to F. S. Crawford's Engineering Note M5, University of California Radiation Laboratory, Berkeley, 1956 (unpublished).

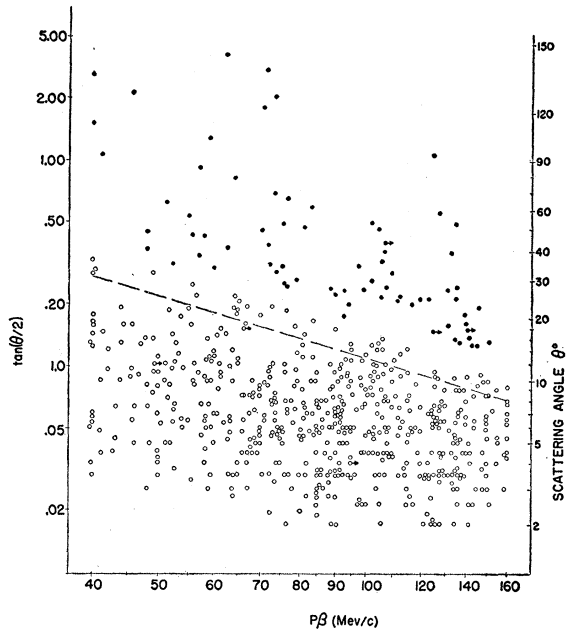


FIG. 1. Diagram showing $\tan(\theta/2)$ ($\theta$=spatial scattering angle) as a function of $P\beta$ of 625 "elastic" scatterings obtained with 1164 $K_L$ mesons. The dots represent these scatterings exceeding by more than 20% the Coulomb cutoff shown by the dotted line. The arrows indicate cases of decay in flight.

It is to be noted that about 6% of the "elastic" scatterings thus classified reveal a blob at the vertex. Since the formation of a blob requires only a few kev, and its presence is actually correlated with the de-excitation of an emulsion nucleus excited by an incident $K$ meson, we must then consider the scatterings with a blob at the vertex as inelastic. To test this correlation we have compared the percentage of blob cases in other stacks having different degrees of processing and background, and have found that the number of such cases increases considerably in one of these stacks having the heaviest background and the highest ionization. Therefore, it seems that the observation of a blob is rather subjective, and cannot serve as a reliable criterion for the identification of a small energy loss in the scattering process.

We shall start the discussion with the results of "elastic" scattering of 1164 $K_L$ mesons. Along a total track length of 40.2 meters, we have observed 625 scatterings in the energy region 20–80 Mev. The results are shown in Fig. 1 where we have plotted $\tan(\theta/2)$ ($\theta$=spatial scattering angle) against $P\beta$ in Mev/$c$, deduced from the remaining range after the scattering. The value of scattering angle $\theta$ is also indicated on the other axis. The cases marked by an arrow correspond to decays in flight; in these cases, only a lower limit was assigned to $P\beta$ for that event. The dots represent those scatterings exceeding by more than 20% the Coulomb cut-off angle shown by the dotted line.

In Fig. 2, we present histograms of the over-all range distributions of the $K_L$ mesons. Histogram (a) gives the distribution of 65 $K_L{}^+$ scatterings having angles greater than the Coulomb cutoff (cases marked by dots in Fig. 1); histogram (b) represents the distribution of 408 $K_L$ scatterings having their angles below the Coulomb cutoff (open circle cases in Fig. 1). For comparison, we have also presented in histogram (c), 661 $K_L$ mesons which do not have any appreciable scattering at a remaining range greater than 3 mm ($P\beta \geq 40$ Mev/$c$). The probable range deduced from the latter histogram is $R=5.75\pm0.38$ cm which corresponds to a momentum $341\pm7$ Mev/$c$ in agreement with the expected momentum of the beam.

An inspection of these histograms shows a striking skewness toward the lower-range region. In order to see if this is simply caused by the fact that these cases had already suffered some inelastic scatterings before being picked up for scanning, we have traced back all $K$ mesons having an over-all range less than 3 cm to the entrance edge of the emulsion, and have not found any evidence supporting this assumption. Therefore, it is believed that the skewness of the distribution is most probably related to the characteristics of the beam.

If we compare these three histograms, we see that histogram (b) is essentially identical to histogram (c); this gives a strong indication that the energy loss involved among the cases of small scattering angle is in

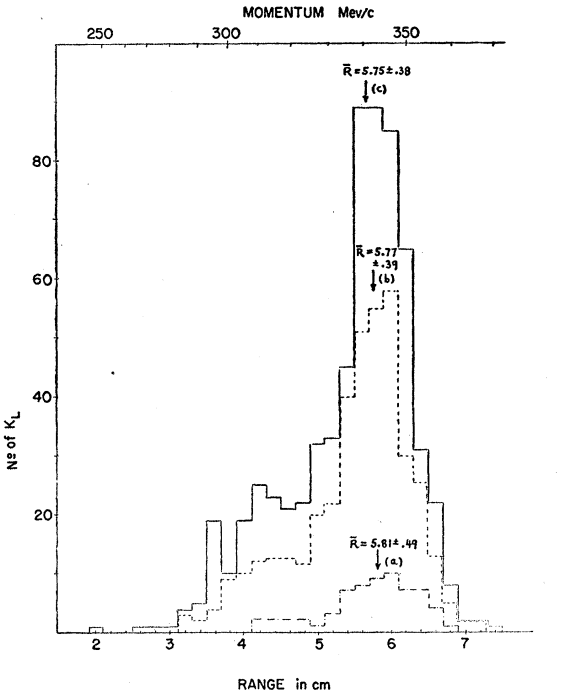


FIG. 2. Over-all range distribution of $K_L$ mesons. Histogram (a) gives the distribution of 65 $K_L$ mesons having scatterings greater than the Coulomb cutoff (cases represented by dots in Fig. 1), (b) represents that of 408 $K_L$ mesons having scatterings below the Coulomb cutoff (open circles of Fig. 1), and (c) represents that of 661 $K_L$ mesons having no appreciable scatterings at a remaining range >3 mm.

reality quite small, on the average, probably not exceeding 1 Mev. On the contrary, histogram (a), corresponding to the large scattering angles, is significantly broadened in comparison with (c); this can be attributed to the fact that some scatterings of this group are actually inelastic, although no energy loss was visibly detected; the percentage of these cases is estimated to be about 12% of the total number in this group, assuming an energy loss of ~5 Mev.

## IV. COMPARISON BETWEEN SCATTERINGS OF $K_L$ AND $\tau$ MESONS

A similar analysis of "elastic" scatterings was carried out with $\tau$ and $\tau'$ mesons found in the present work. In an attempt to compare these results with the $K_L$ mesons discussed above, we have included in our data 179 $\tau$ and $\tau'$ mesons obtained from the Richman group of the Radiation Laboratory, Berkeley. These events were found by this group in connection with a systematic study of abundances of $K^+$ mesons[12]; the scanning method used was the same as the one used here. The additional scattering data from these events were obtained in the following way; all the $\tau$ and $\tau'$ mesons of the Berkeley stack were rescanned starting from the ending of each track to a residual range exceeding 6 cm and all scatterings were recorded during the course of rescanning in the same way as before. Altogether 236 "elastic" scatterings were obtained in a total track length of 9.77 m. The results are presented in Fig. 3 using a similar plot as for the $K_L$ (Fig. 1).

If we compare the results on large-angle scatterings

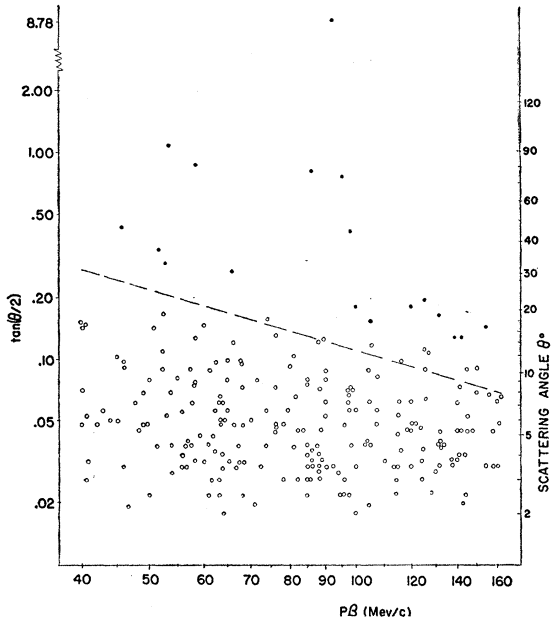


FIG. 3. Diagram showing $\tan(\theta/2)$ ($\theta$=spatial scattering angle) against $P\beta$ of 236 "elastic" scatterings of 276 ($\tau+\tau'$) mesons.

[12] Birge, Perkins, Peterson, Stock, and Whitehead, Nuovo cimento 4, 834 (1956).

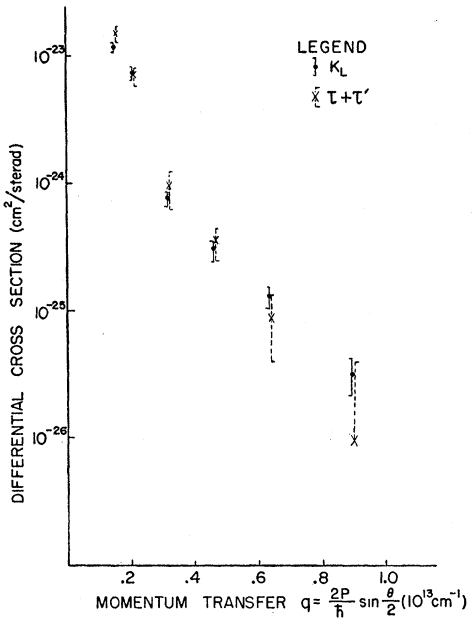


FIG. 4. Comparison between differential cross sections for "elastic" scatterings of $K_L$ and ($\tau+\tau'$) mesons. Correction has been made for geometrical loss of scattering angles due to 2° cutoff of projected angle.

for $K_L$ and ($\tau+\tau'$), we obtain the values given in Table II. The mean free path thus defined is, within statistical error, the same for $K_L$ and ($\tau+\tau'$) mesons.

We can also compare their differential cross sections expressed in terms of the momentum transfer $q=(2P/\hbar)\sin(\theta/2)$. The use of $q$ as a parameter proves particularly convenient for the present purpose, for it is then possible to make use of all available scattering data covering a wide energy range. It is to be noted that the logarithmic plot of $\tan(\theta/2)$ against $P\beta$ here used is very convenient for the present case, since the loci of equal momentum transfer $q$=const are practically represented by parallel lines leading to a considerable simplification in the analysis of our data. The results thus obtained are shown in Fig. 4. In order to reduce any possible experimental bias against recording small angles, we shall consider only those spatial angles greater than 4°. A correction for geometric loss due to the cutoff of 2° in projected angles was made for each angular interval.

We see that, apart from the last point for $\tau$ and $\tau'$, which is subject to a large statistical error, the two

TABLE II. Comparison of scattering data of $K_L$ and $\tau+\tau'$ mesons.

| | Number of cases | Total track length in 40–80 Mev region | Number of scatterings above Coulomb cutoff | Mean free path |
|---|---|---|---|---|
| $K_L$ | 1164 | 37.03 m | 74 | 50.0± 5.8 cm |
| $\tau+\tau'$ | 276 | 9.45 m | 20 | 47.3±10.5 cm |

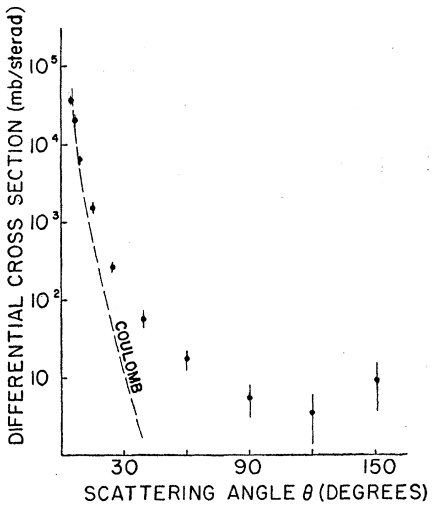


FIG. 5. "Elastic" scattering differential cross sections of $K$ mesons in the interval 30–65 Mev. The dashed line gives the absolute Coulomb scattering differential cross section calculated for the nuclear emulsion using Gaussian form factor.

differential cross sections are essentially indistinguishable. We therefore conclude that the interaction properties of $K_L$ and $\tau$ mesons are identical. This result is in accord with that obtained by the M.I.T. and Harvard group[13] who compared the composition of the $K^+$ meson beam scattered in the backward direction with respect to the incident proton beam with that in the forward direction.

## V. INTERFERENCE BETWEEN NUCLEAR AND COULOMB SCATTERING

From the previous discussion, it follows that we can combine our experimental data on the $K_L$ and $\tau$ meson scattering, and obtain in this way some 861 scatterings, from which we are able to get an accurate angular distribution in a narrow energy interval. We confine ourselves to the region 30–65 Mev, and consider only those spatial angles greater than 4°. For convenience in calculations, we have plotted the angular distribution in terms of the scattering angle $\theta$. The result thus obtained is shown in Fig. 5, where account has been taken of the geometrical correction.

In an attempt to determine the role of the $K^+$-nuclear interaction in elastic scattering observed in photoemulsion, we have compared the observed experimental differential cross section with that expected from the Coulomb scattering alone. Since the composition of emulsion is known from the manufacturer, one can, in principle, calculate the Coulomb cross section knowing the form factor for each element. Unfortunately, investigations on heavy nuclei are still under way, and at this moment it is not possible to carry out a rigorous calculation of the Coulomb scattering. However, if one restricts the investigation to a consideration of small $q$ (momentum transfer) values, it is expected that the Stanford[14] results should give a fairly reliable form factor. This is illustrated in Fig. 6 where we have plotted the average form factor, namely the ratio of the calculated Coulomb cross section to the point-charge cross section for the case of a Gaussian and a modified exponential charge distribution. Since we are primarily interested in the region of scattering angles around 25° ($q=0.478\times10^{13}$ cm$^{-1}$ for an average momentum of 216 Mev/$c$) where the interference between the Coulomb and nuclear scattering is expected to be the most pronounced, we see that the difference between these two form factors is not critical for this investigation.

According to the Stanford results, the Gaussian form factor is preferable to the modified exponential, and so we shall use the former in the present calculation of the Coulomb cross section; the results thus obtained are shown in Fig. 5 by the dashed curve. It is to be noted that the Coulomb cross section plotted in this figure is an absolute value directly deduced from the composition of the emulsion (Ag, Br, C, N, O); no normalization was made to match any experimental points.

We see that the measured differential cross section at 5° is actually lower by a factor ~2.2 in comparison with the calculated Coulomb cross section. On the other hand at $7\frac{1}{2}$° the experimental differential cross section [$(2.10\pm0.02)\times10^{-23}$ cm$^2$/steradian] agrees perfectly well with the calculated Coulomb cross section ($1.98\times10^{-23}$ cm$^2$/steradian). This indicates that our data at 5° are probably still biased against some scattering angles. Nevertheless, the excellent agreement we have

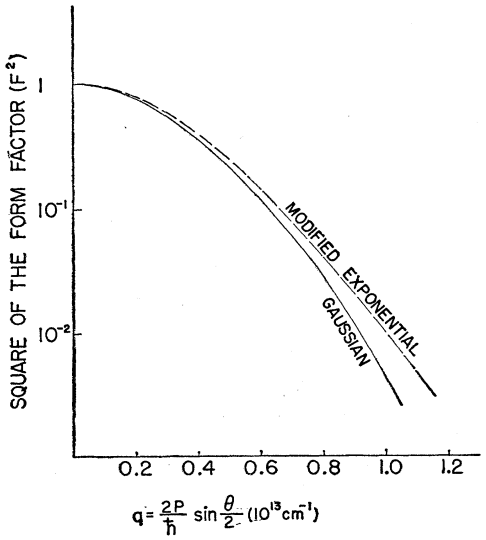


FIG. 6. Square of form factor $F^2$ as a function of momentum transfer $q$. The values $F^2$ are obtained by dividing the calculated Coulomb scattering cross section by the point-charge cross section. The two curves represent, respectively, the Gaussian and the modified exponential distribution.

[13] Widgoff, Shapiro, Schluter, Ritson, Pevsner, and Henri, Phys. Rev. 104, 811 (1956).

[14] R. Hofstadter, Revs. Modern Phys. 28, 214 (1956).

observed at $7\frac{1}{2}°$ between the experimental cross section and the absolute value of the calculated cross section leads us to believe that the data beyond this angle are probably free from any appreciable bias. Consequently, a comparison between the experimental data and the calculated Coulomb curve at and beyond $7\frac{1}{2}°$ should give decisive information on the nature of the interference between the Coulomb and the nuclear scattering.

The fact that all the experimental points are definitely above the Coulomb cross section and that the ratio of the two cross sections increases monotonically with the angle leads to the conclusion that the interference between the Coulomb and the nuclear scattering is constructive; in other words, the nuclear potential felt by the $K^+$ meson is repulsive.

It is to be noted that the experimental cross section at 40° is ~68 times higher than the Coulomb cross section. It is therefore reasonable to consider that all scatterings greater than 40° are due to nuclear interaction. Finally, we have still to decide if those scatterings accepted as "elastic" according to our experimental criteria are in fact coherent in the strict sense of the term; we shall discuss this point in the following.

## VI. OPTICAL MODEL ANALYSIS

It is well known that the optical model introduced by Fernbach *et al.*[15] has achieved a remarkable success in explaining the characteristic features of nuclear scattering. The chief merit of this method lies essentially in the fact that by regarding the nucleus as a dispersive sphere with a characteristic index of refraction related to a complex potential, the problem of scattering is then analogous to that of a classical optical scattering problem. Consequently, a complete solution of the problem can be rigorously treated by the usual procedure of partial wave analysis. The phase shifts thus involved can be evaluated by the KWB method which has the advantage of being insensitive to the detailed shape of the boundary and thus with an appropriate choice of the radius, a uniform form factor can be used for the nuclear density. The application of the optical model to $K^+$ scattering has recently been discussed by Costa and Patergnani[16]; we refer to this paper for the details of the method.

To analyze our data, we limit ourselves to the following forward angles: $7\frac{1}{2}°$, 10°, 15°, and 25°; the data at 5° has been discarded because of the possible experimental bias discussed above. We have tried to fit our data with the absolute differential cross section calculated according to the phase-shift optical model, by using different values of the real part of the nuclear potential. The neglect of the imaginary part is justified by the fact that its contribution to the coherent scattering in the present case amounts to only a few millibarns/steradian.

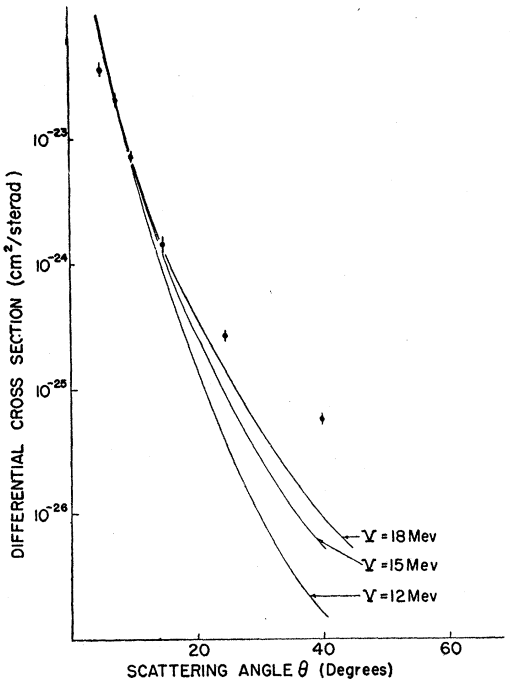


FIG. 7. Phase-shift optical-model analysis of "elastic" scattering data. The curves give absolute differential cross sections calculated for heavy elements of the emulsion assuming a real nuclear potential $V=+12$, $+15$, and $+18$ Mev, respectively.

Three trials have been made by assuming a real nuclear potential equal to $+12$, $+15$, and $+18$ Mev respectively. Calculations were made with the heavy elements of the emulsion Br and Ag, the contribution of light elements being estimated at less than 5%; the results are shown in Fig. 7. The potential $+12$ Mev seems to be too small to match the points at 10°, while the curves corresponding to $+15$ and $+18$ Mev are practically inseparable up to 10°. The best fit according to our data corresponds to a real potential between $+15$ and $+18$ Mev.

## VII. BORN APPROXIMATION APPROACH

The use of the Born approximation in the analysis of $K^+$ scattering was first proposed by Osborne[17] and considered independently by Ravenhall.[18] This method has proven a most valuable tool in the investigation of scattering problems. However, while it gives satisfactory results in the elastic scattering cross section for light elements, it encounters serious difficulties when applied to heavy elements. Since the great majority of elements constituting the emulsion are heavy nuclei, i.e., Br and Ag, one may ask if the use of the Born approximation for photoemulsions is well justified. In the present case, the average value of the parameter $Ze^2/\hbar v$ assumes a value 0.76 which is not small in comparison with unity, as required for the validity of

[15] Fernbach, Serber, and Taylor, Phys. Rev. **75**, 1352 (1949).
[16] G. Costa and G. Patergnani, Nuovo cimento **5**, 448 (1957).
[17] L. S. Osborne, Phys. Rev. **102**, 296 (1956).
[18] D. G. Ravenhall (private communication).

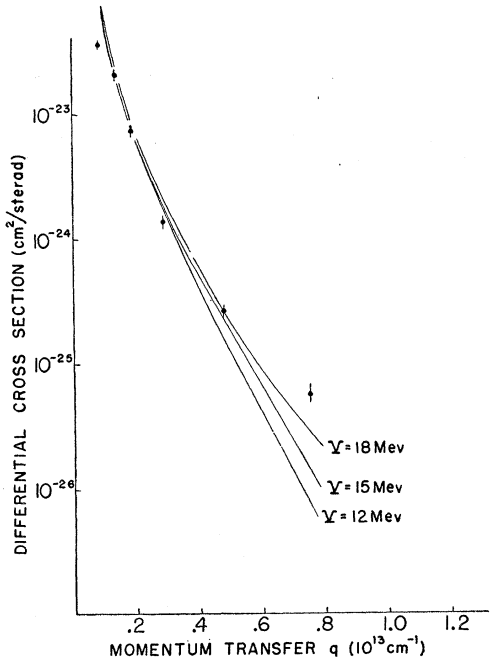


FIG. 8. Born-approximation analysis of "elastic" scattering data. The three curves correspond to the same nuclear potential $V=+12$, $+15$, and $+18$ Mev as in the optical model. The differential cross sections are given in terms of $q$ instead of scattering angle $\theta$.

the Born approximation.[19] None the less, in virtue of the simplicity of its application, it is worth attempting a similar analysis of our data by this method; we can in this way compare the result with that obtained from the optical model.

Contrary to the approach made by Osborne, we consider it better to confine ourselves only to the coherent scattering as in the case of the optical model, and to express the differential cross section in terms of a potential $V$ without making any *a priori* assumptions on the relation between the elementary $K^+-p$ and $K^+-n$ cross sections. For an element of charge $Ze$ and nuclear radius $R$, we have

$$\left(\frac{d\sigma}{d\Omega}\right)_{\text{coherent}}=\left[\frac{2m_KZe^2}{(\hbar q)^2}+\frac{2m_KR^3}{3\hbar^2}V\right]^2F^2(q),$$

where $e$, $\hbar$ are universal constants, $m_K$ the $K$ meson mass, $q$ the momentum transfer, and $F$ the form factor.

In Fig. 8, we present the curves obtained with $V=+12$, $+15$ and $+18$ Mev; here again, we have plotted the absolute cross sections calculated for the heavy elements Br and Ag of the emulsion. These curves are plotted against $q$ instead of $\theta$, but the scale has been so chosen that a direct comparison can be made between Figs. 7 and 8 notwithstanding the different parameters used.

[19] See N. F. Mott and H. S. W. Massey, *The Theory of Atomic Collisions* (Clarendon Press, Oxford, 1949), p. 126.

## VIII. DISCUSSION OF THE RESULTS OF THE ANALYSIS

Referring to Figs. 7 and 8, we see that in general the Born approximation cross section is systematically higher than that of the optical model; this seems to be principally due to the choice of the form factor. The Born approximation cross section is very sensitive to the form factor, especially for large $q$ values; consequently, the slight difference we have observed between the two calculations cannot be considered as a serious discrepancy.

However, we must bear in mind that any calculated coherent scattering cross section should not exceed the experimental cross section in the region we are considering, $\theta\leq 25°$ (the point at 5° being set aside), since the experimental "elastic" scattering data contain both coherent and incoherent events. When we take this into consideration, the $+18$-Mev potential seems to be too high and the best fit occurs probably for $V\simeq+15$ Mev.

From the real part of the $K^+$-nucleus potential it is, in principle, possible to deduce the elementary $K^+$-nucleon scattering amplitude in the forward direction. The relationship is that of the well-known optical theorem:

$$\frac{V(2E-V)}{2m_Kc^2}=\frac{3}{2}\left(\frac{\hbar^2}{r_0^3m_K}\right)\bar{f}^b(0),$$

where $E$ is the total energy of the $K$ meson outside the potential well $V$, $m_K$ its mass, $r_0=1.25\times10^{-13}$ cm the nuclear radius parameter, and $\bar{f}^b(0)$ the average forward scattering amplitude for the nucleons bound to the nucleus,

$$\bar{f}^b(0)=[Zf_p{}^b(0)+Nf_n{}^b(0)]/(Z+N),$$

where the suffixes $p$ and $n$ refer to proton and neutron.

Since we are primarily interested in the scattering amplitude $\bar{f}(0)$ for the $K^+$ free nucleon in the center-of-mass system, an appropriate correction to the $\bar{f}^b(0)$ value is necessary. The relationship between $\bar{f}(0)$ and $\bar{f}^b(0)$ is

$$\bar{f}(0)=\left(\frac{M}{m_K+M}\right)\bar{f}^b(0),$$

where $M$ is the nucleon mass.[20] With $V\simeq+15$ Mev, we find $\bar{f}^b(0)\simeq0.3\times10^{-13}$ cm and $\bar{f}(0)\simeq0.2\times10^{-13}$ cm which corresponds to an average total cross section for free $p$ and $n$ of $\bar{\sigma}\simeq5$ mb (this assumes $f_p=f_n$ and an isotropic scattering in the c.m. system).

To obtain more definitive information concerning the elementary $K^+-p$ and $K^+-n$ scattering amplitudes, we must make some further assumptions. The assumption that the scattering is confined to $S$ waves implied above seems reasonable in light of the energy region

[20] We are indebted to Dr. Charles Goebel for having pointed out to us this correction, which had not been taken into account by the Bologna and Padova groups in their investigation on the same subject.[2,5]

under consideration. It appears to us, as it has to many others, that the next simplest assumption one can make is that of charge independence: the $K^+$-nucleon system can exist in either the isospin $T=0$ or $T=1$ states. If we assume a first approximation that the scattering exists only in the $T=1$ state, then $f_p=2f_n$ and we find for the free proton amplitude $f_p=0.26\times10^{-13}$ cm which corresponds to a total cross section $\sigma_p=[2A/(A+Z)]^2\bar{\sigma}$ $\simeq$9 mb where $A=95$, $Z=42$ are the average atomic number and charge of the emulsion nuclei. It is worth noting that this value seems in agreement with that deduced from the $K^+-p$ scattering as quoted by the Bologna[2] and Padova[5] groups. However, the assumption of scattering only in the $T=1$ state implies the ratio $R=\sigma(\text{charge exch.})/\sigma(\text{inel.})$ equal to $\frac{1}{5}$; this is not in agreement with the data we have observed in the present study (see Sec. X).

If we now allow the existence of scattering in both $T=0$ and $T=1$ states, the ratio $R$ can be expressed as follows:

$$R=\frac{\frac{1}{4}(a_1-a_0)^2}{a_1^2+\frac{1}{4}(a_1+a_0)^2}=\frac{1-2x\cos\phi+x^2}{5+2x\cos\phi+x^2},$$

where $x=|a_0/a_1|$ is the ratio of absolute values of the scattering amplitudes $a_0$ and $a_1$ in $T=0$ and $T=1$ states, respectively, and $\phi$ is the relative phase between $a_0$ and $a_1$. In Fig. 9 we have plotted $x$ *versus* $|\phi|$ for three different values of $R=0$, 0.1, and 0.2. It follows that in order to obtain agreement with our experimental value of $R<\frac{1}{10}$ (see Sec. X), one must allow a superposition of $T=0$ and $T=1$ states under the assumption of $S$-wave scattering only. We shall consider this point in more detail subsequently.

## IX. INELASTIC SCATTERING

Following the discussion on the coherent scattering, we can now attempt a more objective distinction between the "elastic" and "inelastic" scatterings. We have seen that all coherent scattering is expected to take place in the forward direction and that for angles greater than 60° ($q=1.11\times10^{13}$ cm$^{-1}$), the form factor $F^2$ is already so small (see Fig. 6) that any scattering beyond this angle must be considered as incoherent, in the strict sense of the term.

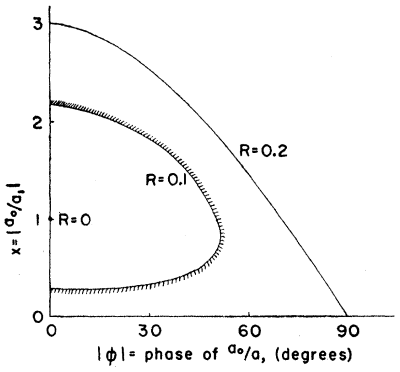


FIG. 9. Curves showing values of $x=|a_0/a_1|$ and $|\phi|$ phase between $a_0$ and $a_1$ for $R=0$, 0.1, and 0.2. The amplitudes $a_0$ and $a_1$ are the $S$-wave scattering amplitudes for states of isotopic spin $T=0$ and $T=1$, respectively; $R$ is the ratio of charge-exchange cross section to inelastic cross section.

From the experimental point of view, we have to distinguish two categories of incoherent scattering:

1. *Obvious inelastic events.*—To these belong those cases which were recognized without ambiguity as such on the basis of our criteria stated above (Sec. II). We have found 12 cases in the energy region 30–65 Mev. Actually all these cases occur at large angles, greater than 45°. The lower limit of energy loss detected among these cases is 7% of the incident energy.

2. *Possible inelastic events.*—These cases were initially classified as "elastic" cases in Sec. II, but were classified *a posteriori* as incoherent cases. To estimate the number of those cases, we take the difference between the experimental differential cross sections and the calculated coherent differential cross sections (see Fig. 7). It is to be noted that the principal contribution to this difference occurs in the vicinity of 40°, since at angles $\theta\geq60°$ all the events can be considered as inelastic, and in the region of 25° the incoherent cross section is practically negligible in comparison with the coherent cross section. This is a consequence of the Born approximation where $\sigma(\text{incoherent})\sim[1-F^2(q)]$, with $F^2(q)\simeq1$ for $\theta=40°$. The number of incoherent cases thus estimated for $\theta\geq40°$ is $28\pm2$.

Therefore, we have altogether $40\pm6$ inelastic scatterings. This leads to a mean free path for incoherent scattering in emulsion of $67.7\pm10$ cm and an average cross section per nucleon $\bar{\sigma}(\text{incoherent})=7\pm1$ mb.

From the optical model point of view, the incoherent scattering constitutes only a part of the total absorption which, in turn, is connected to the imaginary part of the nuclear potential. Since in our case other processes contributing to the absorption of $K^+$ mesons, namely charge-exchange scattering, are negligible in the energy region 30–65 Mev as discussed in the next section, we therefore deduce the imaginary part of the nuclear potential from the incoherent scattering cross section and find $V_{\text{im}}\simeq3.6$ Mev. Figure 10 shows the angular distribution of the 40 inelastic scatterings as deduced from our analysis. The distribution appears to be anisotropic, the greatest contribution to the anisotropy arising from the region around 40°. The number of events in this region was estimated by a subtraction process using our calculation of the coherent scattering cross section. In this calculation we have neglected the imaginary part of the potential. Ravenhall has demonstrated that the inclusion of this part can lead to an enhanced coherent scattering in just this region.[21] We therefore cannot put too great an emphasis on the point

[21] D. G. Ravenhall, *Proceedings of the Seventh Annual Rochester Conference on High-Energy Nuclear Physics, 1957* (Interscience Publishers, Inc., New York, 1957).

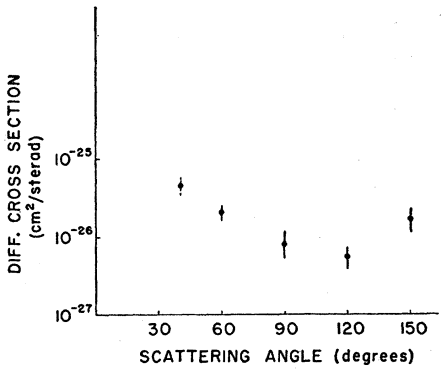


FIG. 10. Angular distribution of incoherent scattering in the interval 30–65 Mev. The point at 40° is obtained by a subtraction process. If one assumes an isotropic distribution, the average differential cross section is ~18 mb/steradian.

at 40°, and can only conclude that an isotropic distribution cannot be ruled out (we would like to comment that the inclusion of the imaginary part of the potential does not seem to appreciably influence our previous conclusions concerning the real part of the potential). If we assume an isotropic distribution for our inelastic scattering, the corresponding differential cross section is found to be ~18 mb/steradian.

The most characteristic feature we have observed with the 12 "inelastic" scatterings of case (1) is the following: Only a relatively small energy loss is involved in the process in contrast with the large momentum transfer implied by the scattering angle. Figure 11 gives the distribution of energy loss for all incoherent cases (the 12 obvious "inelastic" events are cross-hatched in the figure). It seems that about 75% of these events have an energy loss less than 10% of the incident energy.

It is in principle possible to relate the observed incoherent cross section per nucleon to the elementary cross sections as $\bar{\sigma}(\text{incoherent})=(Z\sigma_p\eta_p+N\alpha\sigma_p\eta_n)/(Z+N)$ if a single-particle interaction model is valid, where $\eta_{p,n}$ represents the fraction of collisions allowed by the Pauli principle and $\sigma_n=\alpha\sigma_p$, the parameter $\alpha$ being determined by detailed assumptions concerning the elementary interaction. With the assumption of charge independence for the $K$-nucleon interaction, $\alpha=1$ if the scattering proceeds through the state of isotopic spin $T=0$ while it is $\frac{1}{5}$ for the state with $T=1$ (we include charge exchange). The determination of the parameter $\eta$ depends on detailed assumptions concerning the nuclear model used in the calculation and the energy of the incident $K$ mesons in the nucleus. The most obvious model to use in such a calculation is a Fermi gas model or some variation thereof. Such calculations were originally done for the $\pi$-nucleus case by Johnson[22] and specifically for the $K^+$-nucleus case by the Bologna group[2] and the Padova group.[5] To proceed with such a calculation, a form for the differential cross section in the $K^+$-nucleon c.m. system must be assumed; the simplest assumption is one of isotropy, but others may be made. The principal features arising from such a calculation can be discussed on qualitative grounds.

The principal relations involved in this consideration are the conservation laws of energy and momentum. If the subscript 0 refers to the initial state, the conservation of energy yields

$$\omega_0-\omega=\Delta E+(1/2M)(P^2-P_0^2),$$

where $P$, $P_0$ are the final and initial nucleon momenta (in the nuclear well) and $\Delta E\geq 0$ is the energy difference between initial and final nuclear states. Since the Pauli principle requires that $P^2-P_0^2>P_F^2-P_0^2$ ($P_F\equiv$maximum Fermi type energy), the collision is inelastic. In fact, a large percentage of the collisions will be quite inelastic as can be seen qualitatively from considerations of the degenerate Fermi-gas model. With a maximum Fermi energy of 22 Mev, about $\frac{1}{2}$ of the collisions will be with nuclei whose Fermi energy is below 14 Mev. Thus, if the momentum conservation can be satisfied, $\Delta\omega=\omega_0-\omega\gtrsim 8$ Mev for about $\frac{1}{2}$ of the *a priori* available interactions (for $\Delta E=0$, which is quite unlikely). Consideration of momentum conservation shows that it is easier to satisfy the Pauli principle $[|\mathbf{P}|>P_F\ (\max)]$ for final-state $K$ mesons in the backward hemisphere with appreciably reduced energy. The considerations are quite sensitive to the incident $K$ meson energy. This is most easily seen by allowing the $K$ meson incident energy to become quite small, in which case energy conservation shows that a large number of interactions will be forbidden by the Pauli principle; in fact, the main contribution coming from the allowed interactions should be quite inelastic with protons near the top of the Fermi momentum sphere, while momentum conservation will discriminate against forward scattering angles.

The lack of small angle inelastic scattering is qualitatively in agreement with the experimental observations;

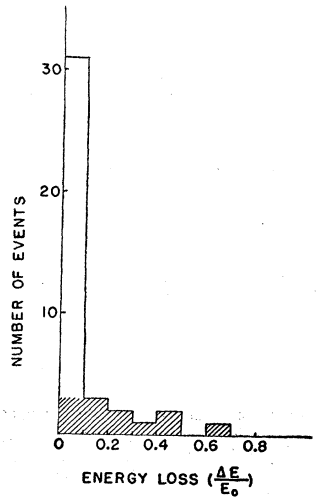


FIG. 11. Histogram showing the distribution of energy loss in the incoherent scatterings of $K_L$ mesons in 30–65 Mev energy region. Obviously inelastic events are represented by cross-hatched area.

[22] M. H. Johnson, Phys. Rev. 83, 510 (1951).

however, the degree of inelasticity is not. About 70% of our inelastic events have energy losses less than 5 Mev which is quite inconsistent with that required in the single-particle model. However, we have not yet explicitly allowed for the effect of the repulsive nuclear potential felt by the $K$ meson which serves to reduce the inelasticity. If the asymptotic fractional energy loss is $\delta\omega=(\omega_0-\omega)/\omega_0$, it is related to the calculated fractional loss $\delta\omega'$ as $\delta\omega=[(\omega_0-V)/\omega_0]\delta\omega'$. Since our median incident energy corresponds to 45 Mev and $V\simeq 15$ Mev, $\delta\omega\simeq 0.67\delta\omega'$. It does not appear, however, that this kind of consideration is sufficient to explain the observed low degree of inelasticity for the large percentage of cases, $\delta\omega_{\text{exp}}\simeq 0.1$ while $\delta\omega'\gtrsim(30-20)/30=0.33$ unless the repulsive potential is considerably larger. This latter possibility seems quite unlikely in view of the results obtained from the optical model analysis. The inconsistency of the approach is demonstrated by the following consideration. If we allow for an appreciably larger repulsive potential the effective energy of the $K$ meson at interaction becomes smaller and though this favors small $\delta\omega$ the influence of the Pauli principle becomes much more important. On the other hand, if we assume $T=1$, $\alpha=\frac{1}{5}$, and $\sigma_p\simeq 10$ mb as deduced from the optical model we obtain $\eta_p=\eta_n\simeq 1$ which seems quite unreasonable (it is to be noted that $\eta_p=\eta_n=0.75$ for $\omega_0=100$ Mev). The foregoing discussion is based upon the assumption of $S$-wave scattering in the c.m. system and the high values of $\eta$ thus deduced are insensitive to the mixture of states of isotopic spin $T=0$ and $T=1$. With these qualitative considerations there appears to be no agreement of the single particle model with experimental results. It would thus appear that quite detailed model calculations should be done to compare with the experimental results.

## X. OTHER EVENTS

In this section we present a detailed account of events other than "elastic" and inelastic scatterings. The data given here correspond to a total $K^+$-track length of $\sim$45 m followed in the systematic scanning of our stack alone.

1. *$K^+-p$ collisions.*—Two cases of $K^+$ and free proton collisions have been observed. In each case, the coplanarity as well as the conservation of energy and momentum have been satisfied within very small experimental error. The specifications of these two cases are listed in Table III. Besides these two cases, there was one case of a $K^+$-bound proton collision which was included among the obvious inelastic cases.

TABLE III. Specification of $K^+-p$ collision events.

| | Energy of $K$ at collision (Mev) | Angle of $K$ in c.m. system |
|---|---|---|
| Case I | 33 | 152° |
| Case II | 58 | 157° |

2. *Decays in flight.*—There are 24 decays in flight. All these cases were definitely identified by their decay secondary (one of the decays is a $\tau^+\to\pi^++\pi^++\pi^-$). The lifetime thus deduced is $(1.22\pm 0.25)\times 10^{-8}$ sec. A more detailed discussion of these decays has been published.[23]

3. *Disappearances.*—Out of a total of 11 disappearances in flight listed in Table I, four of the particles were identified as $K$ mesons. In two of these cases, the disappearances occur at a residual range, estimated from the measured $P\beta$ along the track, less than 4 mm from the expected end. These cases can be either decays in flight in which the minimum secondary escapes observation, or charge-exchange scattering of the $K^+$ meson. From the number of positively identified decays in flight quoted in the previous paragraph, and from the percentage of $K_L$ in which we do not see the minimum secondary (see Sec. II), i.e., $\sim$10%, we expect 2–3 decays in flight appearing as disappearances.

4. *Charge exchange.*—During the course of the systematic scanning, some thirty tracks were found to lead to a star without an outgoing $K^+$ meson. For all these events, careful mass measurement was made on the incident track. None of these cases were found to be compatible with a $K^+$-meson interaction in flight. The only possible charge-exchange processes that we should expect to observe are therefore those among the disappearances. As pointed out above, 2 or 3 of these cases may be attributed to decays in flight; the most probable number of charge-exchange scatterings in the energy region which concerns us is 0, while there could be at most 2. We can therefore set an upper limit for the charge exchange cross section compared with the total inelastic scattering (12 obvious cases plus 10 slightly inelastic cases deduced from range considerations of Sec. III) and find

$$\sigma(\text{charge exchange})/\sigma(\text{inelastic})<\tfrac{1}{10}.$$

This result appears to exclude the possibility that the scattering in our energy region proceeds only through the state of isotopic spin $T=1$ for which the ratio $R$ of charge exchange to noncharge exchange is predicted to be $\frac{1}{5}$. It is worth noting that our experimental ratio is, in reality, an upper limit to $R$. Let $x\equiv|a_0/a_1|$ be the absolute value of the ratio of scattering matrix elements in the states of isotopic spin $T=0$ and $T=1$. Then reference to Fig. 9 shows that according to our data, for which $R<\frac{1}{10}$, this ratio $x$ satisfies the inequalities $0.25\leq x\leq 2.18$, and the relative phase $|\phi|$ is less than 53°.

## XI. REMARK ON $K^+$ STARS

We have observed one $K^+$ star (classified among the obvious inelastic scattering cases of Sec. IX.1). Since a $K^+$ star is a rare event (mean free path for $K^+$ star

[23] Fournet-Davis, Hoang, and Kaplon, Phys. Rev. **106**, 1049 (1957).

TABLE IV. Specification of $K^+$ stars. Symbols in parentheses represent alternative possibilities.

| Group | Secondary prongs |
|---|---|
| Dublin[a] | $K^+ + \alpha + \alpha + \alpha$ |
| Göttingen[b] | $K^+ + \alpha + \alpha + \alpha$ |
| Göttingen[b] | $\tau^+ + \alpha + {}^7\text{Li}\ ({}^6\text{Li}) + p(d)$ |
| Rochester (present work) | $K^+ + \alpha + \alpha + \alpha$ |

[a] See reference 24.
[b] See reference 25.

production is ~45 m in our energy region), it deserves a special description. The star, in addition to the outgoing $K^+$ meson, has three evaporation prongs, two of which are emitted nearly in the same direction and are of length 73 $\mu$ and 96 $\mu$, respectively; these two prongs are definitely identified as $\alpha$-particle tracks. The third prong is only 34 $\mu$ long and an unambiguous identification of its nature is not possible; however, from its ionization, it seems to be the track of a particle heavier than a proton. If we assume that this prong is also that of an $\alpha$ particle, then this star can be interpreted as a disintegration of a carbon nucleus into three $\alpha$ particles, by an incident $K^+$ meson of $61\pm10$ Mev. Examples of the tripartition reaction of a carbon nucleus by a $K^+$ meson have already been observed by other groups.[24,25]

A striking feature revealed by the $K^+$-induced stars observed to date is the following: it seems that most of the evaporation prongs are multiply charged. In fact, if we consider the ratio of the $\alpha$ prongs to the total number of branches emitted in a $K^+$ star, we find from the available data listed in Table IV a value exceeding 0.80 in contrast with the ratio $0.39\pm0.02$ found by Page[26] in the investigation of stars induced by nucleons in the energy region around 100 Mev. It is to be noted that the ratio predicted by Le Couteur's theory[27] lies in the range $0.25\pm0.30$.

It is true that the present statistics are still meager, and cannot be regarded as conclusive. None the less, if our conclusion (that the frequency of $\alpha$ particles is comparable to that of other products in $K^+$ stars) turns out to be valid, it is an indication that in nuclear matter the $K^+$ meson prefers to interact with a complex of nucleons rather than with a single bound nucleon. This, in turn, is not inconsistent with what has been observed in the inelastic scattering of the $K^+$ mesons, as discussed in Sec. IX. We therefore consider it of interest to accumulate further information on $K^+$ stars, which could shed some decisive light on the exact nature of the $K^+$-nucleus interaction.

[24] Anderson, Keefe, Kernan, and Losty, Nuovo cimento 4, 1189 (1956).
[25] Biswas, Ceccarelli-Fabbrichesi, Ceccarelli, Gottstein, Varshneya, and Waloschek, Nuovo cimento 4, 1201 (1956).
[26] N. Page, Proc. Phys. Soc. (London) **A63**, 250 (1950).
[27] K. J. LeCouteur, Proc. Phys. Soc. (London) **A63**, 259 (1950).

## XII. SUMMARY

The present study of 1452 $K^+$ mesons in the energy region 30–65 Mev leads to the following conclusions:

The interaction properties of the $K_L$ and $\tau$ mesons are found to be essentially indistinguishable. This result, in conjunction with other well-established properties of equal mass and lifetime, provides further evidence that $\theta$ and $\tau$ are the same particle.

A direct comparison of the experimental differential cross section for the coherent scattering of $K^+$ mesons with the Coulomb cross section has definitely shown that the interference between nuclear and Coulomb scattering is constructive; thus the nuclear potential felt by $K^+$ mesons is repulsive.

In terms of a phase-shift optical-model analysis, the real part of the potential describing the scattering of $K^+$ mesons in emulsion is about +15 Mev, while the imaginary part is about 3.6 Mev. With the assumption of $S$-wave scattering, charge independence, and dominant isotopic spin state $T=1$, application of the optical theorem yields a $K^+-p$ scattering cross section in agreement with that observed from free $K^+-p$ collisions. However, the ratio of charge-exchange cross section to that of noncharge exchange on the above assumption is inconsistent with our observations. We conclude that if the scattering proceeds principally through $S$ waves, a mixture of both $T=0$ and $T=1$ states must be allowed.

The characteristic feature of the inelastic scattering of $K^+$ mesons is the relatively small energy loss in contrast with a large momentum transfer.

## ACKNOWLEDGMENTS

We wish to express our thanks to Dr. E. J. Lofgren of the Radiation Laboratory, Berkeley, for his valuable help in making possible the exposure of our stack to the Bevatron $K^+$ beam. We are grateful to Dr. R. Birge and Dr. M. Whitehead for the loan of their data on $\tau$ mesons. We acknowledge our thanks to Dr. D. Ravenhall, Dr. C. Goebel, and Dr. G. Rawitscher for various stimulating discussions and to Dr. J. Blum for his help in preparing the exposure and the processing. In addition, we acknowledge with pleasure and appreciation the aid of Mrs. V. Miller, Mrs. J. Milks, and Mrs. B. Sherwood in carrying out the scanning with the highest efficiency.